Supplement: Inferring skeletal production from time-averaged assemblages: timing of production pulses is pulled towards the modern times

Adam Tomašových, Susan M. Kidwell, Rina Foygel Barber

3 supplementary tables

2 supplementary figures

Supplementary table 1 - Coordinates and water depths of 15 sites with *Nuculana taphria*. Site ID numbers are those of the Bight'03 survey, which is also the source of data on numbers of living individuals.

Site ID	Region	Sediment type	Depth (m)	Year of sampling	Longitude	Latitude	%sand	Abundance alive	Number of dated shells
4047	San Barbara Shelf	muddy sand	24.7	2003	-119.66209	34.3956	68.86	0	25
4267	San Barbara Shelf	mud	30.6	2003	-119.43346	34.31313	8.41	6	10
4058	San Pedro Shelf	muddy sand	28	2003	-118.079117	33.642617	76.79	1	10
4090	San Pedro Shelf	muddy sand	29	2003	-118.130697	33.659615	74.43	1	10
4122	San Pedro Shelf	muddy sand	48	2003	-118.140479	33.604468	80.24	1	16
4137	San Pedro Shelf	muddy sand	57	2003	-118.011507	33.576949	82.62	0	15
4265	San Pedro Shelf	muddy sand	40	2003	-118.026628	33.591817	73.62	0	25
4290	San Pedro Shelf	sandy mud	23	2003	-118.184554	33.711698	46.51	5	25
4362	San Pedro Shelf	muddy sand	51	2003	-118.248063	33.637183	70.62	0	25
4369	San Pedro Shelf	muddy sand	56	2003	-117.984603	33.575269	78.22	0	10
4036	Sand Diego Shelf	muddy sand	48	2003	-117.305167	32.796183	63.23	1	25
4244	Sand Diego Shelf	sandy mud	57	2003	-117.282	32.682217	49.69	1	5
4248	Sand Diego Shelf	sandy mud	58	2003	-117.281567	32.679167	49.88	2	7
SM41	Sand Diego Shelf	muddy sand	89	2004	-117.32521	32.665986	71.90	0	22
SM50	Sand Diego Shelf	muddy sand	89	2004	-117.31381	32.646066	63.87	0	24

Radiocarbon ages and calibration of AAR ratios

11 specimens of *Nuculana taphria* were selected for AMS ^{14}C dating at the NOSAMS facility, Woods Hole. One specimen yielded post-bomb ^{14}C ages, one specimen represented a significant outlier in AMS-AAR plot, and thus nine specimens were used in calibration. To estimate ages from amino acid racemization (AAR) measured at Northern Arizona University following Kaufman and Manley (1998), the D/L values were raised to a power-law exponent ***e*** estimated with numerical optimization (Tomašových et al. 2014). The calibration curves were constrained to pass through the origin. The D/L of one specimen of *Nuculana elenensis* collected alive was used was used as the D/L value for zero age (Supplementary Table 2).

Supplementary table 2 - Calibration statistics for the rate of amino acid racemization (AAR) based on paired AAR and ^{14}C analyses of two mollusc species. These define a regression line, where the expected age in calendar years (before AD 2003) corresponds to slope*(D/L)^exponent, with a y-intercept of zero. *n* = the number of specimens used for calibration, Adj.R2 = the adjusted coefficient of determination showing the fit strength. The calibration curves were constrained to pass through the origin. The D/L of one specimen of *Nuculana elenensis* collected alive was used was used as the D/L value for zero age. The ages are computed as $b*([D/L]^e - [D/L]_{alive}^e)$, where *b* is a slope, *e* a power-law exponent, with D/L. We note that the slope estimates for *Nuculana taphria* were mistyped in Tomasovych et al. (2014), with correct values shown in this table.

	Amino acid	*n*	Intercept	Slope	Exponent	Adj. R^2	D/L of living specimen
Nuculana taphria	aspartic acid	9	0	327412	3.576	0.985	0.056
Nuculana taphria	glutamic acid	9	0	9408215	3.26	0.952	0.02

Supplementary table 3 - Amino acid racemization data and estimated calendar ages based on radiocarbon calibration. This file is appended as an excel file.

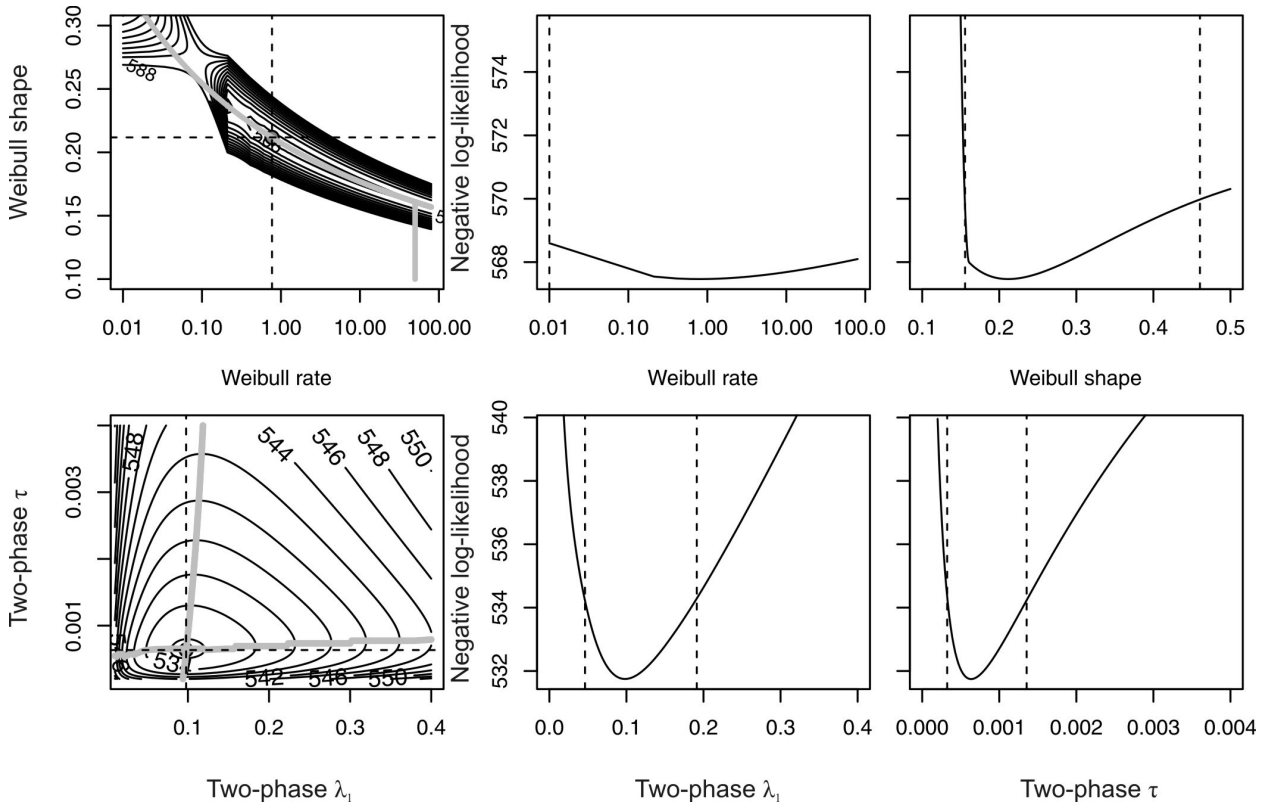

Supplementary figure 1. Left column: Likelihood surfaces show that, using the 51-58 m assemblage, the parameter uncertainties and correlations between estimated parameters are larger in the Weibull (top) than in two-phase (bottom) models. Each data point implicit on this surface shows a fit to the AFD of this assemblage. The contours are separated by two log-likelihoods, and the intersection of the dashed lines represents the maximum likelihood estimate. The gray lines show the location of the likelihood profiles for the two parameters. Middle and right columns: The likelihood profiles representing the ridges on the surface that have the maximum likelihoods for a range of values of two parameters. The Weibull rate parameters has an extremely broad 95% confidence interval (area between the dashed vertical lines in the middle and right graphs). In contrast, the

two-phase model parameters λ_1 and τ are uncorrelated and each has a relatively high precision.

Sensitivity of one-phase and two-phase model parameters to sample size

To assess the effects of sample size on the accuracy and precision of parameter estimates under conditions of constant production, sample sizes range from 25 to 1,000 individuals. We use the values of disintegration and sequestration rates that encompass the range of empirically estimated parameters derived from death assemblages from the Southern California Bight. Both λ and λ_1 vary between 0.05 (half-life = 13.86 years) and 0.0005 (half-life = 1386 years). τ is set to 0.00025 and 0.0001, and λ_2 is set to 0.0001 (half-life = 6,931 years). We simulate AFDs by drawing shell ages (with replacement) from survival functions that specify the probability that a shell has not yet disintegrated at time t of one-phase and two-phase models with predetermined (true) parameters. We then compare the maximum-likelihood parameters estimates obtained from the simulated AFDs with the true parameters. Under constant production, we find that λ is unbiased at small sample sizes (n = 10) and can be estimated with a high precision at n > 50. Estimates of λ_1 in two-phase models have larger dispersion and sample sizes of 50 are needed. As this difference approaches zero, this model will have one phase only, and the estimates of λ_1 under small values can be imprecise. However, estimates of λ_2 in two-phase models are more precise at small sample sizes.

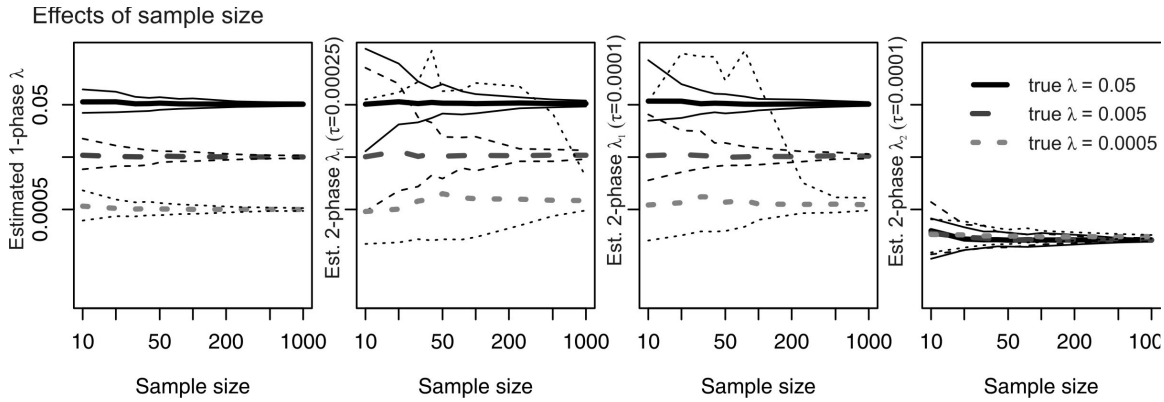

Supplementary figure 2 - A. The effects of (A) sample size on estimates of loss rate in the one-phase (λ, left column) and two-phase models (λ_1 and λ_2, other columns). Smaller sample sizes will suffice to estimate loss rates confidently where the AFD is best explained by a one-phase model of shell loss; sample sizes of 50 shells or more are needed for two-phase model. The left column shows the effects of varying samples size on estimates of λ, two middle columns on estimates of λ_1 under $\tau = 0.00025$ and $\tau = 0.0001$, and the right column on estimates of λ_2, using three true values of λ and λ_1 ranging between 0.05 (solid black lines), 0.005 (dashed dark gray lines), and 0.0005 (dotted light gray lines), and $\lambda_2 = 0.0001$. Thin lines represent 95% confidence intervals on parameter estimates.